The Foerder Institute for Economic Research
at Tel Aviv University

The Eitan Berglas School of Economics

מכון למחקר כלכלי על שם
ד"ר ישעיהו פורדר
על יד אוניברסיטת תל אביב

בית-הספר לכלכלה ע"ש איתן ברגלס

Modelling COVID19: Epidemiological Evidence and Model Misspecifications

Yinon Bar-On, Tatiana Baron, Ofer Cornfeld, Ron Milo and Eran Yashiv

Working Paper No. 15-2020

The Foerder Institute for Economic Research
and
The Sackler Institute of Economic Studies

Modelling COVID19: Epidemiological Evidence and Model Misspecifications*

Yinon Bar-On, Weizmann Institute of Science †

Tatiana Baron, Ben Gurion University ‡ **Ofer Cornfeld, BFI§**
Ron Milo, Weizmann Institute of Science‡

Eran Yashiv, Tel Aviv University and CEPR ¶

October 19, 2020

Abstract

Research in Economics on COVID19 typically posits an economy subject to a model of epidemiological dynamics which is at the core of the analysis. We place this model on the foundations of an epidemiological analysis of the SARS-CoV-2 transmission timescales. We formulate a full model with both epidemiologically-based and clinically-based parameterization. We show that there is often serious misspecification of the model, erroneously characterizing a relatively slow-moving disease, thereby distorting the policymaker decisions towards less severe, delayed intervention. Moreover, the scale of the disease is under-estimated. We also discuss misguided modelling of lockdown policies.

Key words: epidemiological dynamics, COVID19, transmission timescales, optimal policy, public health, disease dynamics and scale, clinical modelling, misspecification.
JEL No. H12,I12,I18, J17.

**We thank Ben Moll and Marc Lipsitch for useful exchanges and seminar participants at UCL and LSE for comments. Any errors are our own.*

†Department of Plant and Environmental Sciences, Weizmann Institute of Science, Rehovot, Israel.

‡Department of Economics, Ben Gurion University, Beer Sheva, Israel.

§BFI, Tel Aviv, Israel.

¶*Corresponding author.* The Eitan Berglas School of Economics, Tel Aviv University, Israel. E-mail: yashiv@tauex.tau.ac.il.

Modelling COVID19: Epidemiological Evidence and Model Misspecifications

1 Introduction

Since March 2020 there has been a rapidly expanding research effort dedicated to COVID19 analysis across disciplines, inter alia, in Economics. A typical analysis posits an economy, which is subject to a model of COVID19 epidemiological dynamics. One type of economic analysis describes a planner problem that seeks to derive optimal policy. This trades off the costs of public health outcomes, such as breach of ICU capacity and death, with the economic costs of suppression policy, including declines in production, consumption, and investment. It leads to the modelling of the well-known concept of "flattening the curve" policy. Another strand of papers models the decentralized economy and the optimal decisions of agents, emphasizing individual epidemic-related behavior as well as externalities. In both cases the dynamics of the disease, as well as its features, like its scale, are at the core of the analysis.

This paper makes two contributions: one is to place this analysis on the foundations of an epidemiological analysis of SARS-CoV-2 properties, particularly, its transmission timescales. The main elements of the ensuing model are two blocks: an infection transmission block, where the number of new cases is determined; and a clinical block, which characterizes the development of symptoms, hospitalization, ICU admission and recovery/death. The former block derives from the epidemiologically-grounded analysis and defines epidemiological dynamics; the latter block models the dynamics within the health system. We offer a complete model of these two different dynamics, including epidemiologically-based and clinically-based parameterizations.

The second contribution is to show that there is often serious misspecification of the model, due to errors in the set-up and in the parameterization, at odds with the epidemiological evidence. These errors have important consequences for optimal economic planning related to COVID19. In particular, they are manifested in erroneously characterizing a relatively slow-moving disease, thereby distorting the policymaker decisions towards less severe, delayed intervention. Moreover, the scale of the disease is underestimated. The underlying cause for the misspecification is the failure to make the distinction between the epidemiological and clinical aspects of COVID19. Wrong values are assigned to key parameters of disease dynamics, and important parameters are omitted. The mis-specification in question runs deeper than simply assigning questionable values to parameters that are highly uncertain.

Finally, we revisit some prevalent approaches to modelling lockdown

policies, highlighting problems in their main assumptions, and propose alternatives. In particular, the quadratic matching properties, flagged by economists, hold true only in highly unrealistic and implausible lockdown situations.

The analysis points economic researchers at the correct way to model the dynamics of the disease. The analysis may also be useful for other epidemics beyond COVID19, as much of the discussion is pertinent to other forms of infectious diseases. Note, in this context, that the set of epidemics since 1980 is quite large and includes, inter alia, HIV/AIDS, SARS, H5N1, Ebola, H7N9, H1N1, Dengue fever, and Zika. We see the analysis here as complementary to the work of Ellison (2020), who focuses on the importance of the correct modelling of population heterogeneity.

The paper proceeds as follows: Section 2 presents key papers in the Economics literature which are relevant for the current discussion. Section 3 presents the epidemiological analysis of SARS-CoV-2. Section 4 discusses the epidemiological model which ensues and the parameterization that is appropriate to use. Section 5 presents the misspecified model used in part of the Economics literature, its parameterization, and its relation to the epidemiology-based model. Section 6 discusses the repercussions of using the wrong model. Section 7 briefly discusses the modelling of lockdowns. Section 8 concludes.

2 Literature

There has been an explosion of research in Economics on COVID19. Avery et al (2020) provide an early review and Baqaee, Farhi, Mina, and Stock (2020) offer a more recent discussion. Two kinds of papers have been making use of epidemiological models in ways that are relevant for the current analysis.

One is work using the concept of an optimizing planner. The point here is to examine in economic terms the health-related losses due to the pandemic and the economic consequences of public health policy. In this framework an objective function is defined, with values taking into account economic losses and the value of statistical life. Thus, tradeoffs are measured and alternative policies can be evaluated. The planner constraints include, inter alia, the disease dynamics typically examined within the SIR epidemiological model. Prominent contributions include Acemoglu, Chernozhukov, Werning, and Whinston (2020), Akbarpour et al (2020), Alvarez, Argente, and Lippi (2020), Chari, Kirpalani, and Phelan (2020), Farboodi, Jarosch, and Shimer (2020), and Jones, Philippon, and Venkateswaran (2020).

The second kind of work includes papers which tie macroeconomic dynamics to the epidemiological dynamics of the SIR model. These models posit that economic behavior has two-way connections with disease trans-

mission. Notable contributions include Eichenbaum, Rebelo, and Trabandt (2020), and Krueger, Uhlig, and Xie (2020). Within the latter strand, the sectorial model of Kaplan, Moll, and Violante (2020) is notable for its careful analysis.

Depending on the exact formulation, we show below how erroneous use – which has been the case in some, but not all of the papers – might lead to work with misspecified models, with substantial consequences for policy. Two key properties of disease dynamics, its scale and speed, are at the center of misspecification.

3 Epidemiological Analysis of the SARS-CoV-2 Transmission Timescales

At the core of many mathematical frameworks for modeling the spread of infectious diseases such as COVID19, lie key timescales which characterize the transmission of the disease between individuals, as well as its progression within an infected individual. These concepts are at the foundation of the renewal equation approach, advanced by Lotka (1907), and the compartmental model approach, proposed by Kermack and McKendrick (1927). In what follows we present these approaches briefly. For a description of the evolution of the literature and a mathematical treatment of the equivalence of the two approaches, see Champredon, Dushoff, and Earn (2018).

3.1 The Generation Interval and the Renewal Equation

The most basic timescale is known as the generation interval and is defined on an infector-infectee pair as the time passed between their corresponding infections. The exact duration of the generation interval is hard to quantify, since transmission time is not observed. The observed quantity is the serial interval, which measures the time between symptoms onset in the pair. Inferring the generation interval from the serial interval requires knowledge of the incubation period, defined as the time from infection to symptoms onset. These timescales vary significantly between individuals, and are better represented as probability density functions (PDFs). References to key studies and details on these timescales are provided in Bar-On et al (2020).

Once inferred, the distribution of generation intervals is used for modeling the disease by the Lotka-Euler renewal equation (see Lotka (1907)):

$$I(t) = \int_0^\infty I(t-\tau) \cdot \beta(\tau, t) d\tau \tag{1}$$

where $I(t)$ is the number of infected people at calendar time t, and $\beta(\tau, t)$ is the transmission rate of people in day τ after their infection. The latter,

also called the infectiousness profile, is the generation interval PDF, $g(\tau)$, scaled by the reproduction number $\mathcal{R}_t$, which is the average number of people infected by a person:[1]

$$\beta(\tau, t) = \mathcal{R}_t \cdot g(\tau) \tag{2}$$

3.2 The Compartmental Approach

An equivalent modeling approach discretizes the infectiousness profile by splitting it up into distinct compartments – the Exposed (E), Infectious (I), and Resolved (R), namely the Susceptible-Exposed-Infectious-Resolved ($SEIR$) model. An infected individual spends some time in each compartment before moving to the next, and is only infectious when in the I compartment, with a transmission rate of $\beta(t)$. The times spent in the E and I compartments are known as the latent[2] and infectious periods, respectively, and the reproduction number, $\mathcal{R}_t$, is thus $\beta(t)$ times the latter. The $SEIR$ model is described by the following differential equations:

$$\begin{aligned}
\dot{S}(t) &= -\beta(t) \cdot I(t) \cdot S(t) && (3)\\
\dot{E}(t) &= \beta(t) \cdot I(t) \cdot S(t) - \sigma E(t) && (4)\\
\dot{I}(t) &= \sigma E(t) - \gamma I(t) && (5)\\
\dot{R}(t) &= \gamma I(t) && (6)
\end{aligned}$$

where S, E, I and R are the fractions of the population in the respective compartments, $\beta(t)$ is the transmission rate during the infectious period, σ is transition rate from E to I and γ is the transition rate from the I to R. The time spent in the E and I compartments is exponentially distributed with a mean of $1/\sigma$ and $1/\gamma$, respectively. The durations of the latent and infectious period are distributed according to the PDFs:

$$T_L(t) = \sigma e^{-\sigma t};\ T_I(t) = \gamma e^{-\gamma t} \tag{7}$$

Exponentially distributed periods capture the mean but not the mode of the biologically accurate distributions, as most people stay longer than zero time at each stage. Therefore, we split the E and I compartments into two sub-compartments and double the rate of transition. Now, the latent and infectious periods are the sum of the time spent in the E_1 and E_2 or I_1 and I_2 sub-compartments, respectively, and their distributions are thus the sum

[1] We use $\mathcal{R}_t$ for the reproduction number at date t and omit the time subscript when time-variability is not essential for the issue at hand.

[2] Not to be confused with the incubation period, which is the time it takes from infection to symptoms onset.

of exponentially distributed random variables, a special case of the Gamma distribution, known as the Erlang distribution. This type of augmented model is known as the $SEIR$-Erlang model, and the corresponding PDFs for the latent and infectious periods are:

$$T_L(t) = (2\sigma)^2 t e^{-2\sigma t};\ T_I(t) = (2\gamma)^2 t e^{-2\gamma t} \tag{8}$$

The means of these distributions remain $1/\sigma$ and $1/\gamma$, but now the modes are near the means.

4 A Model Based on the Epidemiological Evidence

We analyze the evolution of the disease in two complementary blocks – infection transmission and clinical progression. The infections transmission block is characterized by the SEIR-Erlang model discussed above, reflecting the epidemiological properties of COVID19. The clinical block characterizes the development of symptoms, hospitalization, ICU admission and recovery or death and is needed to describe the dynamics within the public health system.

4.1 The SEIR-Erlang Block

Graphically, this model is represented in panel a of Figure 1.

Figure 1

The following equations describe this block. Throughout, all stock variables are expressed as a fraction of the population.

$$\begin{aligned}
\dot{S}(t) &= -\beta(t) \cdot (I_1(t) + I_2(t)) \cdot S(t) && (9)\\
\dot{E}_1(t) &= \beta(t) \cdot (I_1(t) + I_2(t)) \cdot S(t) - 2\sigma E_1(t) && (10)\\
\dot{E}_2(t) &= 2\sigma E_1(t) - 2\sigma E_2(t) && (11)\\
\dot{I}_1(t) &= 2\sigma E_2(t) - 2\gamma I_1(t) && (12)\\
\dot{I}_2(t) &= 2\gamma I_1(t) - 2\gamma I_2(t) && (13)\\
\dot{R}(t) &= 2\gamma I_2(t) && (14)
\end{aligned}$$

4.2 The Clinical Block

The clinical block describes the clinical progression of the disease and the progression of new cases through the healthcare system, depending on the development and severity of symptoms. We postulate the following. Once infected, a person enters an incubation period , a P state, during which

there are no symptoms, lasting for $1/\theta_P$ on average. Following it, a person either remains asymptomatic (O) or develops symptoms (M). Denote the share of asymptomatic cases by η. The others $(1-\eta)$ develop symptoms, and with probability ξ are hospitalized (H). A given share π of patients develop conditions requiring transition to ICU (denoted X). Once in ICU, a fraction $\delta(\cdot)$ dies. We specify the death probability, once in ICU as:

$$\delta(X(t), \overline{X}) = \delta_1 + \delta_2 \cdot \frac{\mathbf{I}(X(t) > \overline{X}) \cdot \left(X(t) - \overline{X}\right)}{X(t)} \tag{15}$$

where $\overline{X}$ denotes ICU capacity and $\mathbf{I}$ is the indicator function.

At any stage, a person may recover (C). The clinical block is represented graphically in panel b of Figure 1.

The analytical description of the symptomatic branch is:

$$\begin{aligned}
\dot{P}(t) &= \beta(t) \cdot (I_1(t) + I_2(t)) \cdot S(t) - \theta_P \cdot P(t) && (16)\\
\dot{M}(t) &= (1-\eta) \cdot \theta_P \cdot P(t) - \theta_M \cdot M(t) && (17)\\
\dot{H}(t) &= \xi \cdot \theta_M \cdot M(t) - \theta_H \cdot H(t) && (18)\\
\dot{X}(t) &= \pi \cdot \theta_H \cdot H(t) - \theta_X \cdot X(t) && (19)\\
\dot{D}(t) &= \delta(X(t)) \cdot \theta_X \cdot X(t) && (20)
\end{aligned}$$

The parameters $\theta_P, \theta_M, \theta_H$, and θ_X relate to the average time that passes between the stages of infection, symptoms onset, hospitalization, ICU admission, and death, respectively.

4.3 Connection to Economic Analysis

We posit that the number of people who can work daily, $N(t)$, is given by:

$$N(t) = l \cdot \rho \cdot (1 - D(t) - X(t) - H(t) - \phi M(t)) \tag{21}$$

where $0 < l < 1$ is the employment fraction out of the total population, $0 < \rho \leq 1$ is the fraction able to work given any policy restrictions, and $0 \leq \phi \leq 1$ is the fraction of people with symptoms who do not work. If $\phi = 1$, anyone who develops symptoms self-isolates immediately and does not work.

4.4 Parameterization

The parameterization of this model needs to be both epidemiologically- and clinically-based. In Table 1 we present the relevant values for the two blocks, where we rely on the analysis in Bar-On et al (2020) and sources in the epidemiological and medical literatures.

Table 1

Note that:

(i) The transmission rate $\beta(t) = \gamma \cdot \mathcal{R}_t$ depends on the regime – either lockdown – $\gamma \cdot \mathcal{R}_L$, or out of lockdown (work) – $\gamma \cdot \mathcal{R}_W$.

(ii) The implied Infection Fatality Rate (IFR) is 0.8%,consistent with the estimates of the Imperial College COVID19 Response Team (2020).

Additionally, based on Bar-On et al (2020), we set $\delta_1 = 0.5$. In the U.S. economy, ICU capacity is $\overline{X} = 1.8 \times 10^{-4}$, based on an estimate of approximately 58,100 ICU beds by the Harvard Global Health Institute.[3] Finally, following Kaplan, Moll, and Violante (2020), we set $\delta_2 = 0.5$.

5 Alternative Specifications

The overwhelming majority of Economics papers on COVID19 model both clinical outcomes and infections dynamics within a single block. In many cases its calibration is anchored by two numbers that pertain to two separate processes – the spread of the disease and its clinical progression:

a. The reproduction number $\mathcal{R}_t$, often calibrated at 2.50, following various sources, for example CDC estimates.[4]

b. Duration till death. It takes on average 18-19 days to die from COVID19, once one gets infected (Imperial College COVID-19 Response Team (2020)).

We proceed by presenting a widely-used model (SIR) and its calibration, a modification ($SIRD$) designed to better capture the epidemiology of the disease, and then discuss the relations between the different specifications.

5.1 The Widely-Used SIR Model

Economists modelling the dynamics of COVID19 have mostly been using versions of an SIR model with the following structure.

$$\dot{S}(t) = -\beta(t) \cdot I(t) \cdot S(t) \tag{22}$$

$$\dot{I}(t) = \beta(t) \cdot I(t) \cdot S(t) - \gamma I(t) \tag{23}$$

$$\dot{R}(t) = \gamma I(t) \tag{24}$$

Whenever numbers of deceased and recovered are needed the following equations are used:

[3] See https://globalepidemics.org/our-data/hospital-capacity/

[4] https://www.cdc.gov/coronavirus/2019-ncov/hcp/planning-scenarios.html#table-1

$$\dot{D}(t) = \mu \dot{R}(t) \quad (25)$$
$$\dot{C}(t) = (1-\mu)\,\dot{R}(t) \quad (26)$$

where D is deceased, C is recovered and μ is the infection fatality rate.

The resulting prevalent calibration is:

$$1/\gamma = 18 \Longrightarrow \gamma = 1/18$$

$$\beta = \mathcal{R} \cdot \gamma = 2.50 \cdot 1/18 = 0.139$$

Thus:

a. The duration of the disease till death is exactly the duration of the Infected stage, and it is $1/\gamma$.

b. The infection transmission rate β is pinned down by both $\mathcal{R}$ and the length of the infectious stage.

5.2 The SIRD Model

The specification above contradicts two facts established in the epidemiological analysis of COVID19 and shown in Table 1:

a. There is a latency period of around 3 days in which people infected are not infectious.

b. People are infectious for a short period of time (4 days on average), though it may take longer till one recovers or dies.

To tackle the second issue, some economists modify the SIR model, replacing equation (24) by:

$$\dot{R}(t) = \gamma I(t) - \theta \cdot R(t) \quad (27)$$

where θ defines the duration of the resolving stage R. Also, replacing equations (25)-(26), one gets:

$$\dot{D}(t) = \mu \cdot \theta \cdot R(t) \quad (28)$$
$$\dot{C}(t) = (1-\mu) \cdot \theta \cdot R(t) \quad (29)$$

This model is denoted $SIRD$ and is calibrated to match the above targets:

$$\gamma = 1/7$$

$$\theta = 1/11$$

$$\beta = \mathcal{R} \cdot \gamma = 2.5 \cdot 1/7 = 0.357$$

5.3 Relations Between the Specifications

We consider four different model specifications:

a. models (i) + (ii) – the full $SEIR$-Erlang model, discussed above in Section 4; we look at both our preferred specification of two sub-compartments (model i, denoted $SEIR-2$, see sub-section 4.1), and a simpler variant (model ii, denoted $SEIR$, see equations (3)-(6) in sub-section 3.2);

b. model (iii) – the widely-used SIR model parameterization discussed in sub-section 5.1;

c. model (iv) – the $SIRD$ model of sub-section 5.2.

Figure 2 illustrates these different specifications and presents the values given to the key parameters.

Figure 2

The key difference between the models lies in the implied transmission rate β, as seen in the fourth row of the table in Figure 2. Specifications that assume a long infectious period have to posit a low transmission rate β in order to match a particular value of $\mathcal{R}$, while specifications that assume the epidemiologically-grounded short infectious period, posit a higher β.

The separation of the infection generation block from the clinical block lies at the heart of the differences between the widely-used SIR parameterization and the benchmark $SEIR-2$ model or its simplified counterpart $SEIR$. Targeting two separate timescales with one parameter (γ) has important implications. The $SIRD$ model presented in sub-section 5.2 alleviates the problem somewhat by adding a parameter θ thus enabling separate targeting of $\mathcal{R}$ and duration-till-death.

6 The Implications of Misspecification

We explore the implications of the different dynamics inherent in the models shown in Figure 2.

6.1 Key Features of the Disease

The length of the infectious period, governed by γ, has important effects on implied epidemic dynamics. At the start of the epidemic $S(t) \simeq 1$. The SIR model of sub-section 5.1 has the following approximate solution for I using equation (23):

$$I(t) = I(0)\, e^{\lambda t} \tag{30}$$

where $\lambda = \beta(t) - \gamma = \gamma(\mathcal{R}_t - 1)$.

As seen in Figure 2, different calibrations imply very different disease growth rates. While all models, except for SIR, imply daily disease growth

rates of $17\% - 21\%$ (doubling every $3.2 - 4.2$ days), the widely-used SIR implies a growth rate of 8% (doubling every 8.3 days). Panels a and b in Figure 3 illustrate the development of the disease, as measured by the stock of infectious and exposed people (panel a) and hospitalized in ICU (panel b), under the different models.

Figure 3

a. *Slow disease in the widely-used SIR.* From Figure 3 and Table 1 one sees that a specification with a very long infectious period – the SIR model with $\gamma = 1/18$ – implies a much lower transmission rate β and therefore much slower disease progression; the epidemic is spread out in time, and the maximal number of infected at a given point in time reaches 24% of the population on day 120. It takes almost 330 days for the epidemic to die out.

b. *Faster dynamics in SEIR and SIRD.* By contrast, specifications with a relatively short infectious period, the $SEIR$ models and the $SIRD$ model, imply much faster dynamics. The epidemic starts aggressively and cases rise very fast, reaching the peak on days 59 (for $SEIR$), 56 (for $SEIR-2$), and 49 (for $SIRD$). The epidemic also dies off quickly; there are hardly any people in I after day 120, and the entire episode ends twice as fast as under the SIR model calibration.

c. *Scale of the disease*. In the $SEIR-2$ model with two sub-compartments, more people are infected before herd immunity is attained, and so a higher level of disease is reached. At the peak, the number of infectious/exposed people reaches over 27% of the population (a difference of 3.5% relative to the other models, or 11.6 million people in the case of the U.S). This can be seen in the higher peak of the red lines in I and in X in Figure 3 and in the numbers presented in panel c of Table 2.

d. *Effects on ICU utilization.* Panel b of Figure 3 shows that with a slow moving disease, implied by a long infectious period, ICU capacity is breached on day 82, and peak demand exceeds capacity by a factor of 7, whereas in the epidemiological-grounded model it is breached much earlier, on day 41, and peak demand exceeds capacity by a factor of 14.

These numbers pertain to an unmitigated disease and do not correspond to real world data, where suppression measures have been undertaken.

e. *Role of the latent period.* Ignoring the short latent period (E), as in SIR and $SIRD$, has moderate effects on epidemic dynamics. In $SIRD$, relative to the two $SEIR$ models, the epidemic develops somewhat faster at the beginning, because there is no delay between the moment a person becomes infected and the moment he or she starts spreading the disease.

f. *The role of sub-compartments.* Division of I and E into sub-compartments and their number has some effects on both the speed and the scale of the

disease. Using only one compartment for I and E implies dynamics such that most of the people exposed become infectious immediately and most of the infected recover immediately. This is counter-factual. When the disease is rising, each compartment and sub-compartment is more populated that the compartment following it.

The underlying dynamics (not shown) are that in the $SEIR$ model, the disease slows down with the number of E sub-compartments and speeds up with the number of I sub-compartments; when both E and I sub compartments are increased, the combined effect depends on model parameters. Specifically, in COVID19 where $\gamma < \sigma$, the disease speed is faster when increasing the number of both sub-compartments in E and I.

g. *Implications for initial conditions.* Under equal initial conditions, it takes much more time for the epidemic to gain pace under the widely-used SIR model than under $SEIR-2$. One can try to 'circumvent' this problem by assuming a higher initial seed of the infection. Panel c of Figure 3 compares the $SEIR-2$ model with initial seed of 10^{-4} and the SIR model with initial seed of 10^{-2}. It shows that assuming a higher initial seed does place SIR on the same timescale as $SEIR-2$ in terms of the length of the entire episode and timing of the peak. However, two problems remain. First, at peak, the implied number of infectious individuals is still way lower under SIR, which distorts the problem of a policymaker constrained by a number of hospital/ICU beds. Second, assuming a seed of 1% of the population implies, in terms of the U.S. economy, that the epidemic has started when over 3.3 million people were infected. This is a highly implausible assumption, given actual data on known cases and on deaths.

6.2 Initial Disease Dynamics and the Reproduction Number

As mentioned, the Lotka–Euler equation is used in epidemiology to study disease growth. The reproduction number, $\mathcal{R}$, can be extracted from the initial growth rates of the disease. Following Wallinga and Lipsitch (2007), the characteristic equation of Lotka-Euler is given by:

$$1 = \int_0^\infty e^{-\lambda\tau} \cdot \beta(\tau) d\tau \tag{31}$$

Using equations (1), (2), (30), and (31) they get:

$$\frac{1}{\mathcal{R}} = \int_0^\infty e^{-\lambda\tau} g(\tau) d\tau \tag{32}$$

The term on the right-hand side of equation (32) is both the Laplace transform of the function $g(\tau)$ and the moment generating function $M(\lambda)$ of the distribution $g(\tau)$.

Thus:

$$M(\lambda) = \int_0^{\infty} e^{\lambda\tau} g(\tau) d\tau \tag{33}$$

and so:

$$\mathcal{R} = \frac{1}{M(-\lambda)} \tag{34}$$

Wallinga and Lipsitch (2007) go on to show the explicit expression for $\mathcal{R}$ using different formulations of $g(\tau)$.

For the case of the SIR model and $SIRD$:

$$\mathcal{R} = 1 + \frac{\lambda}{\gamma} \tag{35}$$

For $SEIR$:

$$\mathcal{R} = \left(1 + \frac{\lambda}{\gamma}\right)\left(1 + \frac{\lambda}{\sigma}\right) \tag{36}$$

For $SEIR$ model with m, n sub-compartments it is given by (using equation 4 in Wearing et al (2005)):

$$\mathcal{R} = \frac{\lambda\left(\frac{\lambda}{\sigma m}+1\right)^{m}}{\gamma\left(1 - \left(\frac{\lambda}{\gamma n}+1\right)^{-n}\right)} \tag{37}$$

Once the value of λ is known, Figure 2 provides numerical values for all other parameters needed to compute $\mathcal{R}$.

One concludes that even if one were to recover the reproduction number $\mathcal{R}$ from data on disease speed λ, the incorrect value of γ still leads to erroneous results for β.

6.3 Implications for an Optimizing Planner Problem

In order to illustrate the consequences of the wrong parameterization of γ, in particular for the number of deaths and breach of ICUs, we use an optimizing planner model. The planner minimizes the following loss function:

$$\min \int_{t=0}^{\infty} e^{-rt}\left(\frac{Y(t)}{N(t)}\left(N^{ss} - N(t)\right) + \chi \dot{D}(t)\right) dt \tag{38}$$

The loss function is minimized in PDV terms (r is the discount rate) over the infinite horizon, where at finite point T_V (set at 540 days) the vaccine is found and the pool of susceptibles drops to zero, so that the disease stops growing. The loss function includes both lost output Y, due to a decline in employment N relative to steady state, and the value (with parameter χ)

of lost life. The latter is affected by the breach of ICU modelled in equation (15) above.

To work within a realistic but simple set-up, we let the planner decide on when to start and stop a full lockdown. In Alon et al (2020) we allow for alternative lockdown strategies and for more choices of timing. We use the parameterization of Table 1 and start with $\mathcal{R}_t$=2.50 consistent with the findings of Jones and Villaverde (2020). Following the review of the literature in Karin et al (2020) and their estimates, we use $\mathcal{R}_L = 0.80$ for the lockdown period and $\mathcal{R}_W = 1.50$ thereafter. Referring to the U.S. economy, we use $\rho = 0.7$ for the fraction of workers able to work in a lockdown, using evidence cited in Alon et al (2020), and $\chi = 85.7$ for the value of lost life following Hall, Jones, and Klenow (2020) and Greenstone and Nigam (2020).[5]

We solve the planner problem for the optimal start and stop dates of lockdown with the afore-cited SIR model plugged into the infection transmission block. We subsequently compare results across two scenarios using the same policy plan: (i) The true model of the disease is in accordance to plan ('planned'), and (ii) The true model of the disease is $SEIR-2$ ('realized'). Such comparison gives a sense of the cost of errors made when using the wrong model and parameter values.

Figure 4

In both scenarios, lockdown is set between days 75 and 147. In the first scenario, following the blue lines, one can see that in lockdown a small breach of ICU capacity occurs; in panel b of Figure 4, X attains $2.4 * 10^{-4}$ while $\overline{X} = 1.8 * 10^{-4}$. This is followed by a decline in infections. Following the release there is a smaller second wave, which does not breach ICU capacity. The disease declines to below 0.5% on day 454 and the cumulative death toll is 0.43%, 1.43 million people in U.S. terms. Loss is 0.42 in PDV, annual GDP terms, out of which 0.06 is loss of output, and 0.36 is loss of life.

What is the planner doing? A long lockdown to suppress the disease until a vaccine is found is too expensive. Therefore the planner tries to minimize death by trying to avoid both breaching the ICU limit and overshooting the herd immunity threshold ($S^* = 0.66$) for $\mathcal{R}_W = 1.50$). Optimal lockdown balances moderate ICU breach with moderate overshooting

[5]

$$\begin{aligned}\chi &= \frac{\text{expected years remaining} \cdot \text{value of statistical life}}{\frac{Y}{POP}} \\ &= \frac{14 * 400,000}{65,351} = 85.7\end{aligned}$$

($S(T_V) = 0.48$ vs. $S^* = 0.66$). The two-wave pattern is consistent with outcomes observed during the 1918 influenza pandemic in the locations that implemented NPIs early on (Hatchett, Mecher, and Lipsitch (2007)).

In the second scenario, the planner is mistaking the speed of the disease and thus the severity of the situation. Most of the outbreak happens before lockdown is imposed. The epidemic rages unmitigated and declines to below 0.5% on day 81. The overshooting is huge, with $S(T_V) = 0.11$ vs. $S^* = 0.66$. Following the red lines, one can see the enormous breach of ICU capacity; X attains $24 * 10^{-4}$, ten times the value above. The number of deaths increases to $12,962$ per 1 million, out of which $5,859$ per 1 million are due to the breaching of ICU capacity, and the cumulative death toll is 1.29%, 4.28 million people in U.S. terms. Loss is 1.18 in annual GDP PDV terms, out of which 0.08 is loss of output and 1.1 is loss of life. The latter is a tremendous loss, caused by the misperception of the dynamics of the disease.

Three remarks are in place. One is that in Alon et al (2020) we show that much more favorable outcomes, with much lower death numbers, can be attained when allowing the planner more choices of lockdown strategies. The cost of mis-specification, though, remains high. The second, and related to the first, is that in the real world, U.S. death numbers are currently almost $160,000$, or 0.05%, an order of magnitude lower than even the relatively 'benign' first scenario above. This is so because U.S. policymakers have imposed longer lockdowns than the planner above, as they have access to wider policy choices. Third, most papers, which model the SIR-based planner, actually present even higher numbers of deaths, in the order of magnitude of the second scenario above, or worse.

7 Modelling Lockdowns

In this section we question the assumptions underlying prevalent models of lockdown policy, a non-pharmaceutical intervention (NPI) used worldwide to control the spread of the disease. In lockdown, work and consumption activities, which involve social interactions, are restricted. We use the $SEIR$ model to offer a brief discussion of the modelling of these policies.

In what follows, all variables are expressed in stocks, rather than fractions of the total population (denoted by POP). We assume that when the policymaker locks down a share of $(1 - \alpha)$ of the population this part is completely isolated. The dynamics over time depend on the way the lockdown is modelled. We discuss two such ways.

7.1 Lock-and-Hold

Consider a lockdown imposed at time t_0. The part of the population that is locked is chosen at random and held locked down throughout the intervention; namely a "lock-and-hold." At time t_{0-}, before lockdown, the following equations hold true with corresponding initial conditions:

$$\begin{aligned}
\dot{S}(t) &= -\beta(t) S(t) \frac{I(t)}{POP} && (39)\\
\dot{E}(t) &= \beta(t) S(t) \frac{I(t)}{POP} - \sigma E(t) && (40)\\
\dot{I}(t) &= \sigma E(t) - \gamma I(t) && (41)\\
\dot{R}(t) &= \gamma I(t) && (42)\\
S(t_{0-}) &= S_0, E(t_{0-}) = E_0, I(t_{0-}) = I_0, && (43)\\
R(t_{0-}) &= R_0, L(t_{0-}) = 0,\\
S + E + I + R + L &= POP
\end{aligned}$$

where L denotes the pool of people under lockdown.

After lockdown, at time t_{0+}, the same dynamic equations (39)-(42) hold true. Since public spaces, public transportation, and other human gatherings are occupied by the fraction of the population not locked, this implies an effective transmission rate of $\alpha \cdot \beta(t)$. The chance of meeting an infector is computed out of the active population, $\alpha \cdot POP$. Therefore, the dynamics of new cases is governed by $\dot{S}(t) = -\alpha \cdot \beta(t) S(t) \frac{I(t)}{\alpha \cdot POP}$ which reduces to equation (39). However, initial conditions are altered so as to reflect the lockdown:

$$\begin{aligned}
S(t_{0+}) &= \alpha S_0, E(t_{0+}) = \alpha E_0, I(t_{0+}) = \alpha I_0, && (44)\\
R(t_{0+}) &= \alpha R_0, L(t_{0+}) = (1-\alpha) POP,\\
S + E + I + R + L &= POP
\end{aligned}$$

By reducing the size of the interacting population, the system is placed on a new epidemiological track for the duration of the lockdown, described by the same dynamic equations with different initial conditions.

The effective reproduction number is defined by $\mathcal{R}_e = \mathcal{R}_t \cdot \frac{S(t)}{POP}$. Lockdown controls the spread of the disease by reducing $S(t)$, and if $\mathcal{R}_e$ is driven below 1, the disease declines for the duration of the lockdown. As long as one is willing to pay the price of forgone output, such a lockdown, being intuitive and clear, allows to suppress or control the disease, while waiting for cures and vaccines.

7.2 Lock-and-Reshuffle

The quadratic nature of equation (39) above is reminiscent of matching processes in search models. Some papers in Economics have proposed to use it so as to exploit this dynamic property. Note, however, that the implicit assumption here is that not only is $(1-\alpha)$ of the population locked, but that it is released, reshuffled with the rest of population, sampled randomly again, and locked again. We call this type of lockdown "lock-and-reshuffle." In order for the quadratic reduction in cases to occur, one needs to ascertain that at each instant exactly a share α of all susceptibles and a share α of all infected are active. The disease dynamics are:

$$\begin{aligned} \dot{S}(t) &= -\alpha\beta(t)\alpha S(t)\frac{\alpha I(t)}{\alpha POP} \\ &= -\beta(t)\alpha^2 S(t)\frac{I(t)}{POP} \end{aligned} \tag{45}$$

In such a case, by paying the linear cost of lockdown, one gains a quadratic reduction in the spread of the disease. Though an attractive feature of the model, such policy is highly unrealistic and impractical. It assumes that all workers are interchangeable or that they can be organized in homogenous groups for sampling. Such mechanisms do not respect the differentiation between essential and nonessential workers and between workers who can work remotely and those who cannot. Moreover, the fact that personal history does not influence the chances of release contradicts basic principles, such as fairness, stability, and predictability. We believe that "lock and reshuffle" is not a realistic policy instrument and that lockdowns should be modelled in more sensible ways. One of the options is the "lock-and-hold" model presented above.

8 Conclusions

The paper has shown how dynamics in COVID19 should be modelled and parameterized based on epidemiological and clinical analyses. Duration of the infectious stage is crucial for implied disease dynamics. The widely-used SIR model makes a grave mistake and extends the infectiousness period, distorting policymaker decisions towards less severe and delayed interventions. It makes a smaller omission by ignoring the latent stage and not considering sub-compartments. Tweaking the initial seed in the baseline SIR model to correct its timescale requires implausible assumptions and is misleading in terms of the predicted burden on the constrained public health system.

We use the epidemiologically-grounded model in companion work (Alon et al (2020)) to explore an optimal planner model with two dimensions –

the degree of lockdown policies and their timing. The emerging optimal policy is quite different from the one proposed thus far in the Economics literature.

References

[1] Acemoglu, Daron, Victor Chernozhukov, Ivan Werning, and Michael D. Whinston, 2020. "A Multi-Risk SIR Model with Optimally Targeted Lockdown" NBER Working Paper No. 27102.

[2] Akbarpour Mohammad, Cody Cook, Aude Marzuoli, Simon Mongey, Abhishek Nagaraj, Matteo Saccarolak, Pietro Tebaldi, and Shoshana Vasserman, 2020. "Socioeconomic Network Heterogeneity and Pandemic Policy Response," BFI, working paper 2020-75.

[3] Alon, Uri , Tanya Baron, Yinon Bar-On, Ofer Cornfeld, Ron Milo, and Eran Yashiv, 2020. "COVID19: Looking for the Exit," working paper, available at

https://www.tau.ac.il/~yashiv/LSE%20June%20paper.pdf

[4] Alvarez, Fernando, David Argente, and Francesco Lippi, 2020. "A Simple Planning Problem for COVID-19 Lockdown," NBER Working Paper No. 26981.

[5] Avery, Christopher, William Bossert, Adam Clark, Glenn Ellison, and Sara Fisher Ellison, 2020. "Policy Implications of Models of the Spread of Coronavirus: Perspectives and Opportunities for Economists," **Covid Economics** 12, 1 May.

[6] Baqaee, David, Emmanuel Farhi, Michael Mina, and James H. Stock, 2020. "Policies for a Second Wave," **Brookings Papers on Economic Activity**, **Summer 2020 Special Edition: COVID-19 and the Economy**, **forthcoming.**

[7] Bar-On, Yinon, Ron Sender, Avi Flamholz, Rob Phillips, and Ron Milo, 2020. "A Quantitative Compendium of COVID-19 Epidemiology," arXiv:2006.01283; available at https://arxiv.org/abs/2006.01283

[8] Champredon, David, Jonathan Dushoff, and David J.D. Earn, 2018. "Equivalence of the Erlang-distributed SEIR Epidemic Model and the Renewal Equation," **SIAM Joural of Applied Math** 78, 6, 3258–3278.

[9] Eichenbaum, Martin S., Sergio Rebelo, and Mathias Trabandt, 2020. "The Macroeconomics of Epidemics," NBER working paper No. 26882.

[10] Ellison, Glenn , 2020. "Implications of Heterogeneous SIR Models for Analyses of COVID-19," NBER Working Paper No. 27373

[11] Farboodi, Maryam, Gregor Jarosch, and Robert Shimer, 2020. "Internal and External Effects of Social Distancing in a Pandemic," NBER Working Paper No. 27059.

[12] Greenstone, Michael and Vishan Nigam, 2020. "Does Social Distancing Matter?" BFI working paper.

[13] Hall, Robert E, Charles I. Jones, and Peter J. Klenow, 2020. "Trading Off Consumption and COVID-19 Deaths,"**Minneapolis Fed Quarterly Review** 42, 1, 2-14.

[14] Hatchett, Richard J., Carter E. Mecher, and Marc Lipsitch, 2007. "Public Health Interventions and Epidemic Intensity During the 1918 Influenza Pandemic," **Proceedings of the National Acadmey of Sciences (PNAS)** 104,18, 7582–7587.

[15] Imperial College COVID-19 Response Team, 2020. "Report 13: Estimating the number of infections and the impact of non-pharmaceutical interventions on COVID-19 in 11 European countries," available at https://dsprdpub.cc.ic.ac.uk:8443/bitstream/10044/1/77731/10/2020-03-30-COVID19-Report-13.pdf

[16] Johns Hopkins University CSSE, 2020. "2019 Novel Coronavirus COVID-19 (2019-nCoV) Data Repository," Center for Systems Science and Engineering.

[17] Jones, Callum J., Thomas Philippon, Venky Venkateswaran, 2020. "Optimal Mitigation Policies in a Pandemic: Social Distancing and Working from Home," NBER Working Paper No. 26984.

[18] Jones, Charles I. and Jesus Fernandez-Villaverde, 2020. "Estimating and Simulating a SIRD Model of COVID-19 for Many Countries, States, and Cities," NBER Working Paper No. 27128.

[19] Kaplan, Greg, Ben Moll, and Gianluca Violante, 2020. "The Great Lockdown: Macroeconomic and Distributional Effects of Covid-19," Manuscript, University of Chicago.

[20] Karin, Omer, Yinon Bar-On, Tomer Milo, Itay Katzir, Avi Mayo, Yael Korem, Avichai Tendler, Boaz Dudovich, Eran Yashiv, Amos J Zehavi, Nadav Davidovitch, Ron Milo and Uri Alon, 2020. "Adaptive cyclic exit strategies from lockdown to suppress COVID-19 and allow economic activity", MedRxiv, available at https://www.medrxiv.org/content/10.1101/2020.04.04.20053579v4.full.pdf

[21] Kermack, William O., and Anderson G. McKendrick, 1927. "A Contribution to the Mathematical Theory of Epidemics," **Proceedings of the Royal Society London**. Ser. A., 115, 700–721.

[22] Krueger, Dirk, Harald Uhlig, and Taojun Xie, 2020. "Macroeconomic Dynamics and Reallocation in an Epidemic," NBER Working Paper No. 27047

[23] Lotka, Alfred J., 1907. "Relation Between Birth Rates and Death Rates," **Science**, 26, 21–22.

[24] Wallinga, Jacco and Marc Lipsitch, 2007. "How Generation Intervals Shape the Relationship between Growth Rates and Reproductive Numbers," **Proceedings of the Royal Society** 274, 599–604

[25] Wearing, Helen J., Pejman Rohani, and Matt J. Keeling, 2005. " Appropriate Models for the Management of Infectious Diseases," **PLoS Medicine** 2, 7, 621-627.

1 Exhibits

Figure 1: The Model

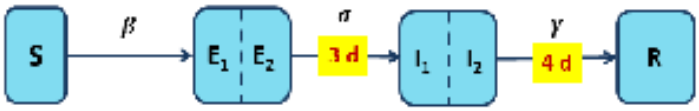

a. The SEIR-Erlang block

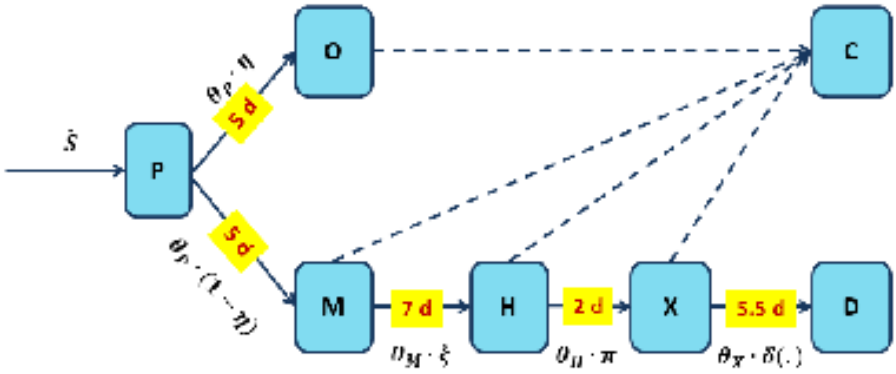

b. The Clinical Block

Table 1 : Epidemiologically-grounded and Clinically-based Parameterization

a. The SEIR-Erlang Block

	Interpretation	**Value range (source)**	**Preferred value**	**Number used**
σ	latent period duration	$3-4$ (Compendium)	3	1/3
γ	infectious period duration	$4-5$ (Compendium)	4	1/4
β	transmission rate			$\gamma \cdot \mathcal{R}$

b. The Clinical Block

	Interpretation	**Value range (source)**	**Preferred value**	**Number used**
θ_P	incubation period	$5-6$ (Compendium)	5	1/5
θ_M	days from symptoms till hospitalization	7 (S1, S2)	7	1/7
θ_H	days in hospital till ICU	2 (S3)	2	1/2
θ_X	days in ICU before death	5.5 (S3, S4)	5.5	1/5.5
η	Prob. to be	$20\%-50\%$ (Compendium)	50%	0.5
	asymptomatic			
ξ	Prob. to get hospitalized when symptomatic	$\frac{\#Hospitalized}{\#Infected}$ $= [2\%-4\%]$ (Compendium)	4%	$\frac{0.04}{1-0.5}$ $= 0.08$
π	Prob. of ICU admission	$10\%-40\%$ (Compendium)	40%	0.4

Notes:

1. Values in third and fourth columns are in days. 2. $\frac{\#Hospitalized}{\#Infected} = \frac{\#Hospitalized}{\#Symptomatic} \cdot \frac{\#Symptomatic}{\#Infected} = \xi \cdot (1-\eta) \implies \xi = \frac{\frac{\#Hospitalized}{\#Infected}}{1-\eta}$

3. Sources:

a. Compendium: Bar-On, Sender, Flamholz, Phillips, and Milo (2020).

b. S1: CDC
https://www.cdc.gov/mmwr/volumes/69/wr/mm6915e3.htm

c. S2: The Lancet
https://www.thelancet.com/action/showPdf?pii=S0140-6736%2820%2930183-5

d. S3: Science
https://science.sciencemag.org/content/early/2020/05/12/science.abc3517/tab-pdf

e. S4: JAMA
https://jamanetwork.com/journals/jama/fullarticle/2765184

Figure 2: Alternative Specifications of the Epidemiological Model

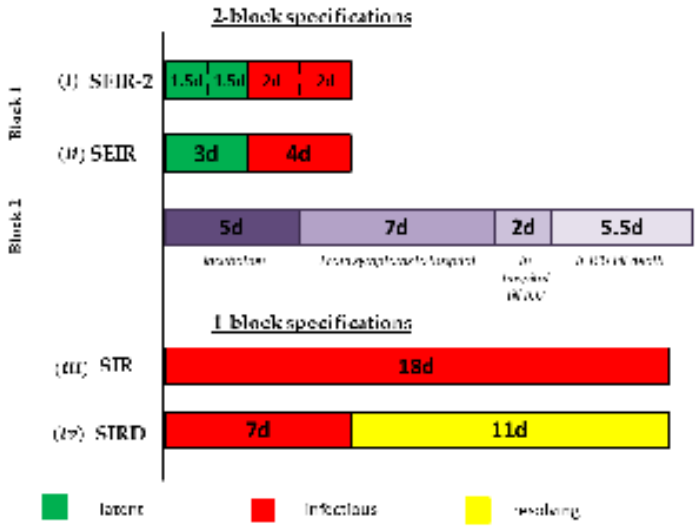

Table 2. Four specifications: parameterizations and properties

	2-block specifications		1-block specifications	
	$SEIR$	$SEIR-2$	SIR	$SIRD$
Panel A: Parameterization				
σ	1/3	1/3	–	–
γ	1/4	1/4	1/18	1/7
θ	$n.a^{(a)}$	$n.a^{(a)}$	–	1/11
β	$\mathcal{R} \cdot 1/4 = 0.625$	$\mathcal{R} \cdot 1/4 = 0.625$	$\mathcal{R} \cdot 1/18 = 0.139$	$\mathcal{R} \cdot 1/7 = 0.357$
$Scale^{(b)}$	$E + I$	$E_1 + E_2 + I_1 + I_2$	I	I
Panel B: Implied exponential growth rate and doubling time				
$\lambda^{(c)}$	0.17	0.18	0.08	0.21
$t^{(d)}$	4.16	3.91	8.32	3.23
Panel C: Herd immunity and disease scale at peak				
S^*	0.4	0.39	0.4	0.4
$Scale^*$	0.23	0.27	0.23	0.23

Notes: 1. We assume throughout $\mathcal{R}$= 2.50. 2. (a) there is no duration for R in these models. (b) scale of the disease - the number of people who are either infectious or exposed (will become infectious). (c) exponential growth rate. (d) doubling time 3. S^*: Herd immunity - the fraction of susceptibles such that the disease scale reaches its peak. For model a without sub-compartments S^*= $1/\mathcal{R}$. In SEIR-2 there is no closed-form expression but $S^* < 1/\mathcal{R}$ 4. $Scale^*$ - scale of the disease at the peak. For the models with no sub-compartments it is $1-\frac{1+\ln(\mathcal{R})}{\mathcal{R}}$. In SEIR-2 there is no closed-form expression but $Scale^* > 1-\frac{1+\ln(\mathcal{R})}{\mathcal{R}}$.

Figure 3: Disease Dynamics

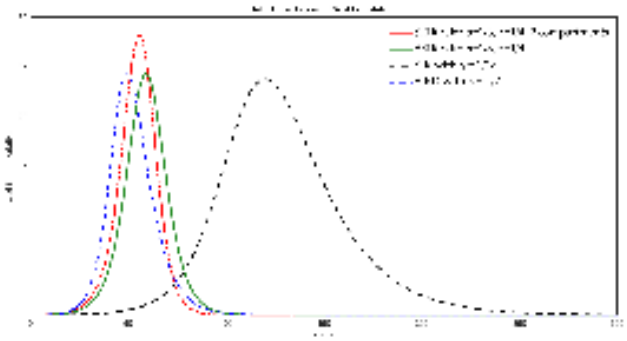

Panel A: The Stock of Infectious and Exposed

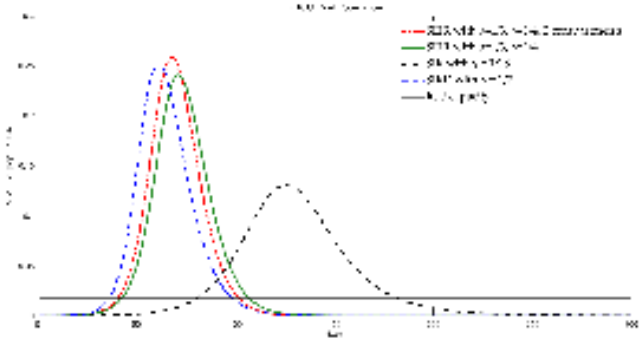

Panel B: In ICU

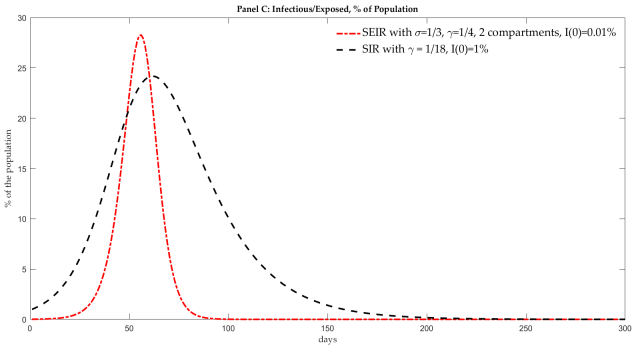

Panel C: Comparing SEIR-2 with seed=10^{-4} and SIR with seed=10^{-2}

Figure 4: Planner Errors

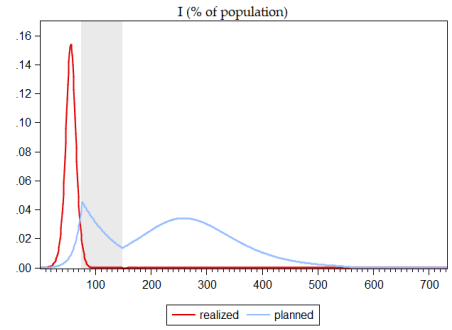

Panel A: The Stock of Infectious and Exposed

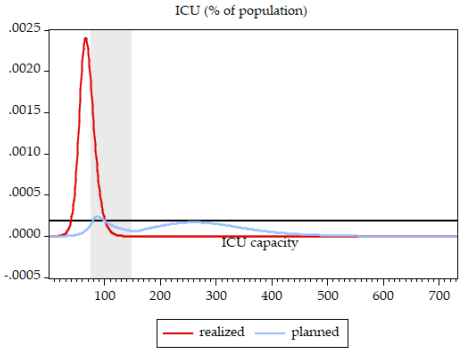

Panel B: In ICU

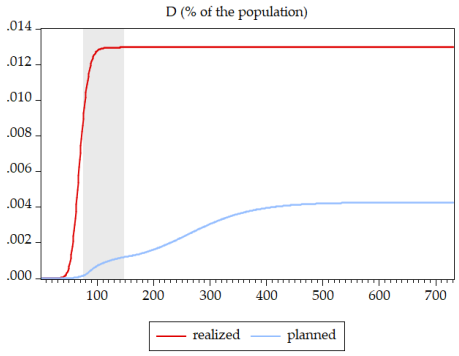

Panel C: Cumulative Deaths

Note: Shaded area indicates lockdown period.